

# Heavy Quark Dynamics in the QGP

V. Greco\*, H. van Hees† and R. Rapp\*\*

*\*Department of Physics and Astronomy, University of Catania,  
Via S. Sofia 64, I-95125 Catania (Italy)*

*†Institut für Theoretische Physik, Goethe-Universität Frankfurt,  
Ruth-Moufang-Str. 1, D-60438 Frankfurt, Germany,*

*\*\*Cyclotron Institute and Physics Department,  
Texas A&M University, College Station, Texas 77843-3366, U.S.A.*

**Abstract.** We assess transport properties of heavy quarks in the Quark-Gluon Plasma (QGP) that show a strong non-perturbative behavior. A T-matrix approach based on a potential taken from lattice QCD hints at the presence of heavy-quark (HQ) resonant scattering with an increasing strength as the temperature,  $T$ , reaches the critical temperature,  $T_c \simeq 170$  MeV for deconfinement from above. The implementation of HQ resonance scattering along with a hadronization via quark coalescence under the conditions of the plasma created in heavy-ion collisions has been shown to correctly describe both the nuclear modification factor,  $R_{AA}$ , and the elliptic flow,  $v_2$ , of single electrons at RHIC and have correctly predicted the  $R_{AA}$  of D mesons at LHC energy.

**Keywords:** Quark-Gluon Plasma, Heavy-Quarks, Relativistic Heavy-Ion collisions, Quarkonia

## INTRODUCTION

One of the most interesting questions in high-energy nuclear physics is about the properties of the hot and dense medium created in ultra-relativistic heavy-ion collisions. Finite-temperature lattice-QCD (lQCD) calculations of strongly-interacting matter predict a phase transition from hadronic matter to a quark-gluon plasma (QGP) at a critical temperature,  $T_c \simeq 170$  MeV [1]. The heavy charm and bottom quarks are particularly valuable probes for the properties of this medium. In the context of QGP physics they are considered heavy because their mass,  $m_Q$ , is large not only with respect to  $\Lambda_{QCD}$  but also to the temperature,  $T$ , of the plasma. This remains true going from SPS to LHC energies spanning a  $T$  range of 200-600 MeV. This property makes the study of heavy quark special, because  $m_Q \gg \Lambda_{QCD}$  allows to determine the initial heavy-quark (HQ) spectra by means of pQCD and makes available an out-of-equilibrium probe; the production time  $\tau_0^Q \ll \tau_{QGP}$  is much smaller than the QGP lifetime. Therefore heavy quarks pass through the entire evolution of the fireball; the HQ equilibration time  $\tau_{eq}$  is of the order of the QGP lifetime but smaller than the light-quark one  $\tau_{eq}^Q \sim \tau_{QGP} \gg \tau_{eq}^q$  which means that in principle they carry more information;  $m_Q \gg T$  has two important implications: on one hand it imposes effective flavor conservation, that in particular holds not only during the QGP phase but also in the hadronization process; on the other hand it implies also that the momentum exchange by collisions  $|q^2| \ll m_Q^2$  (parametrically dominated by elastic scatterings), and the dynamics can be treated as a Brownian motion by means of a Fokker-Planck equation which constitutes a significant simplification of the

study of transport properties. Finally, the three-momentum transfer dominates over energy transfer  $|\vec{q}| \gg q_0 \sim \frac{\vec{q}^2}{m_Q}$  which allows to use the concept of a potential and therefore to link the HQ physics to the studies to of the HQ free energy in IQCD [33]. The latter property allows to employ a finite-temperature  $T$ -matrix approach to study the problem of HQ interactions in the medium providing a consistent framework to evaluate both bound-state and scattering solutions based on a two-body static potential.

The first results at RHIC further enhanced the potential interest in HQ dynamics by showing an unexpectedly strong interaction of heavy quarks with the medium observed through a small nuclear modification factor,  $R_{AA}(p_T)$ , and a large elliptic flow,  $v_2(p_T)$ , of the single electrons,  $e^\pm$ , from semileptonic HQ decays. Before these experimental results such a behavior was considered as an unrealistic upper limit, useful only as a reference [2]. Instead, the prediction of a large  $R_{AA}$  and a small  $v_2$  obtained from gluon Bremsstrahlung from heavy quarks has been in striking contrast with the observations [4, 5]. Furthermore, it has not been possible to observe the expected mass hierarchy in the suppression and its color dependence that would lead to  $R_{AA}(B) > R_{AA}(D) > R_{AA}(h)$  [4]. This was in part due to the rather indirect experimental access to the HQ dynamics through the measurements on the single  $e^\pm$ , which does not allow to disentangle the individual contributions from  $B$  and  $D$  mesons. A first breakthrough in this direction has been possible thanks to the recent preliminary results on  $D$  mesons presented at QM2011 by the ALICE Collaboration [6] which confirm a large suppression of heavy mesons. In these Proceedings we discuss HQ scattering in the QGP focusing on the possibility of resonance scattering with light (anti-)quarks reminiscent of quark confinement. We discuss the comparison of the model with the data at RHIC and the 2007 prediction for LHC.

## RESONANT IN-MEDIUM HEAVY-QUARK SCATTERING

Early approaches to the study of HQ scattering in the medium was carried out using perturbative QCD (pQCD), first using elastic scattering [3] and later based on gluon-bremsstrahlung energy loss and/or including elastic HQ scattering [4, 5]. In such approaches only a moderate decrease of  $R_{AA}$  and a small  $v_2$  of the single electrons from  $D$  and  $B$  decays have been expected in clear disagreement with the experimental observations. Hence non-perturbative approaches are expected to be necessary to explain the strong HQ interaction with the medium. An early suggestion postulated a mechanism via the formation of  $D$ - and  $B$ -meson resonance excitations in the deconfined phase of QCD matter [7, 8]. This idea has first been realized through a non-relativistic effective field theory, modeling colorless (pseudo-) scalar and (axial-) vector  $D$ - and  $B$ -mesons exploiting both chiral symmetry and HQ (spin) symmetry,

$$\begin{aligned} \mathcal{L}_{Dcq} = & \mathcal{L}_D^0 + \mathcal{L}_{c,q}^0 - iG_S \left( \bar{q}\Phi_0^* \frac{1+\gamma \cdot v}{2} c - \bar{q}\gamma^5 \Phi \frac{1+\gamma \cdot v}{2} c + h.c. \right) \\ & - G_V \left( \bar{q}\gamma^\mu \Phi_\mu^* \frac{1+\gamma \cdot v}{2} c - \bar{q}\gamma^5 \gamma^\mu \Phi_{1\mu} \frac{1+\gamma \cdot v}{2} c + h.c. \right) \end{aligned} \quad (1)$$

The fields,  $(\Phi^*) \Phi$ , represent (*anti*)- $D$ -mesons, transforming as isospinors under isospin rotations and with the usual  $\mathcal{L}_{c,q}^0$  free terms for quarks and  $D$ -mesons; see Ref. [7] for more details.

The interaction terms in Eq. (1) were evaluated to leading order in  $1/m_c$  according to HQ effective theory (HQET). The main parameter is given by the coupling  $G_{S,V}$  varied to allow for widths of the  $D$ -meson spectral functions of 300-500 MeV, to approximately cover the range suggested by effective quark models. It is important to note that we assume the  $D$ -meson resonances,  $m_D = 2.0$  GeV to be located above the  $c - \bar{q}$  mass threshold,  $m_c + m_q = 1.5$  GeV, which renders them accessible in  $c - \bar{q}$  scattering processes. The situation is quite different for (bound) meson states (i.e., below the anti-/quark threshold), where the resonant part of the scattering amplitude cannot be probed through  $c + \bar{q} \rightarrow c + \bar{q}$  interactions (even for resonance masses close to threshold, thermal energies of anti-/quarks imply that the average collision energy is significantly above the resonance peak).

We find that the presence of these resonances at moderate QGP temperatures substantially accelerates the kinetic equilibration of  $c$ -quarks as compared to using perturbative interactions. We have concentrated on the charm-quark case, but completely analogous expressions apply to the bottom sector. These approaches have been used in 2006 to make predictions for the case of Au+Au at RHIC energies, and the details are presented in Ref. [8]. The key ingredients are that the transport cross section is appreciably larger than the pQCD ones and a hadronization mechanism that includes quark coalescence [12, 14, 15], leading to an enhancement of both the quark  $R_{AA}$  and  $v_2$  toward a better agreement with the data [8, 16]. Other approaches have consistently pointed out the necessity to go beyond a simple pQCD scheme [17, 18] to account for the observed  $R_{AA}$  even if these studies included coalescence especially in the  $p_T^e \leq 3-4$  GeV region, which translates to  $p_T^D \leq 7-8$  GeV at the meson level. In particular our approach appeared to be the only one able to describe both the small  $R_{AA}$  and large  $v_2(p_T)$  simultaneously. Furthermore a prediction for Pb+Pb collisions at LHC energy has been presented in the last call for prediction proceedings [32] and will be discussed in the following.

## **T-matrix Approach to Heavy-Quark Scattering**

The success of the first applications of the idea of resonant HQ scattering in the medium has lead to a further and more realistic assessment of the existence of resonance scattering. The idea of the existence of resonance scattering is indeed supported by IQCD on the quark correlators for both heavy and light quarks [19] as well as by Non-Relativistic QCD solved on lattice for heavy quarks [20]. They both show the existence of a peak in the spectral function even at temperatures substantially higher than  $T_c$  suggesting the presence of a physical mechanism beyond a simple free scattering.

As mentioned in the introduction, the large HQ mass allows the use of an interaction potential between quarks. This has the advantage that  $T$ -matrix scattering theory becomes applicable, which does not rely on a perturbative expansion but is able to account also for moderate or even strong coupling, where resummations of large diagrams are necessary and realized via the standard ladder sum. An extra benefit is that one can in

principle extract the quark potential from finite-temperature lattice QCD (IQCD), or at least be constrained by IQCD “data” which gives a parameter-free input.

A static heavy-quark light-quark potential,  $V(r)$ , has been used in the vacuum to successfully describe  $D$ -meson spectra and decays [22, 23]. We assume that the effective in-medium potential can be extracted from finite-temperature IQCD calculations of the color-singlet free energy  $F_1(r, T)$  [24, 25] for a static  $\bar{Q}Q$  pair as the internal potential energy by the usual thermodynamic relation [21, 26, 27],

$$U_1(r, T) = F_1(r, T) - T \frac{\partial F_1(r, T)}{\partial T}. \quad (2)$$

For the application as a scattering kernel in a  $T$ -matrix equation, the potential has to vanish for  $r \rightarrow \infty$ . Thus we choose the accordingly subtracted internal potential energy,

$$V_1(r, T) = U_1(r, T) - U_1(r \rightarrow \infty, T). \quad (3)$$

In IQCD simulations one finds that  $U_1(r \rightarrow \infty, T)$  is a decreasing function with temperature which could be associated as a contribution to the in-medium HQ mass,  $m_Q(T) = m_0 + U_1(r \rightarrow \infty, T)/2$ , where  $m_0$  denotes the bare mass. However, close to  $T_c$  the asymptotic value,  $U_1(r \rightarrow \infty, T)$ , develops a pronounced peak structure which is currently not fully understood (possibly related to multiple coupled channel effects). For simplicity, in the current calculation, we assume constant effective HQ masses,  $m_c = 1.5$  GeV and  $m_b = 4.5$  GeV.

We also consider the complete set of color channels for the  $Q\bar{q}$  (singlet and octet) and  $Qq$  (anti-triplet and sextet) systems, using Casimir scaling as in leading-order pQCD,  $V_8 = -V_1/8$ ,  $V_3 = V_1/2$ ,  $V_6 = -V_1/4$ , which is also justified by IQCD calculations of the finite- $T$  HQ free energy [28].

The uncertainties due to the extraction of the potential have a moderate final impact on the agreement with the experimental data, see also Fig.3 (left), while the difference in the transport coefficients going from the internal energy,  $U$ , to the free energy,  $F$ , is quite substantial. However, the successful application to compute quarkonium correlators and HQ susceptibilities lends a-posteriori support (albeit not validation) for the choice of  $U$ , which is not as convincing for  $F$  (cf. Ref. [29]).

The starting point of HQ Brueckner theory is a system of coupled Bethe-Salpeter (BS) and Schwinger-Dyson (SD) equations characterizing the HQ interaction and propagator in the QGP,

$$M = K + \int KGM, \quad \Sigma^Q = \Sigma_g^Q + \int TS^q, \quad S^Q = S_0^Q + S_0^Q \Sigma^Q S^Q, \quad (4)$$

where  $M$  denotes the scattering amplitude between a heavy ( $Q$ ) and a light ( $q$ ) quark or antiquark,  $K$  the two-body interaction kernel,  $G$  the two-particle ( $qQ$ ) propagator,  $S^{Q,q}$  ( $S_0^{Q,q}$ ) the (free) single-particle propagator, and  $\Sigma^Q$  the HQ selfenergy receiving contributions from thermal gluons ( $\Sigma_g$ ) and light quarks (where the latter are computed self-consistently from the heavy-light scattering amplitude). Since we focus on a QGP at zero chemical potential ( $\mu_q=0$ ), all quantities are quark-antiquark symmetric. The predominantly space-like momentum transfer in on-shell scattering of heavy

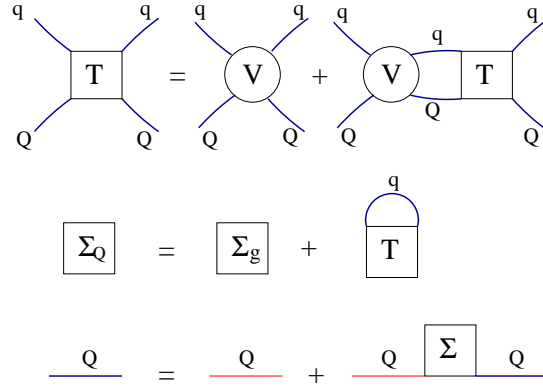


**FIGURE 1.** Diagrammatic representation of the Brueckner many-body scheme for the coupled system of the  $T$ -matrix based on IQCD static internal potential energy as the interaction kernel and the HQ self-energy.

quarks,  $q^2 = q_0^2 - \vec{q}^2 \simeq -\vec{q}^2$ , justifies a static (potential) approximation to its interaction,  $K \approx V$ . This allows to reduce the four-dimensional (4D) BS equation into a 3D Lippmann-Schwinger equation for the  $T$ -matrix, which greatly simplifies its solution. Using azimuthal symmetry and a partial-wave expansion leads to a one-dimensional integral equation for the amplitudes,  $T_l$ , of given angular momentum,  $l$ ,

$$T_l^a(E; p', p) = V_l^a(p', p) + \frac{2}{\pi} \int dk k^2 V_l^a(p', k) G_{Qq}(E; k) T_l^a(E; k, p), \quad (5)$$

where we also indicated the four possible color channels,  $a$ , for  $Q\bar{q}$  (singlet and octet,  $a = 1$  and  $8$ ) and  $Qq$  (antitriplet and sextet,  $a = \bar{3}$  and  $6$ ) states.

The in-medium HQ quasiparticle-dispersion relation is given by

$$\omega_k^Q = \sqrt{k^2 + m_Q^2(T)} + \text{Re} \Sigma_q^Q(\omega_k^Q, k), \quad (6)$$

where it has been assumed that Eq. (4) (middle) can be decomposed into two distinct contributions: a “gluon-induced” one,  $\Sigma_g^Q$ , generating a temperature-dependent mass,  $m_Q(T)$ , and a selfenergy,  $\Sigma_q^Q$ , due to scattering of heavy quarks off thermal light quarks. The former is associated with the long-distance limit of the potential, while the latter is explicitly evaluated from the above heavy-light  $T$ -matrix. To close the system of equations (4) in the quark sector, the analogous system for the light sector is required, which has been solved selfconsistently for  $\Sigma^q$  and  $T_{qq, \bar{q}q}$  in Ref. [21]. Guided by the results obtained there we employ a light-quark propagator (figuring into the second term in Eq. (4) with a constant thermal light-quark mass,  $m_q = 0.25$  GeV, and width,  $\Gamma_q = 200$  MeV =  $-\text{Im} \Sigma^q$ ).

Clearly, the potential approximation is less reliable in the light-quark sector, but it turns out that their in-medium selfenergies (real and imaginary parts), which are needed for the HQ selfenergy, Eq. (4), have a small effect on both the scattering amplitude,  $T_{Qq}$ , and the HQ transport coefficients.

The above system of equations (for  $T$  and  $V$ ) is pictorially represented in Fig. 1 with the upper, middle and lower panel corresponding to Eqs. (4), respectively.

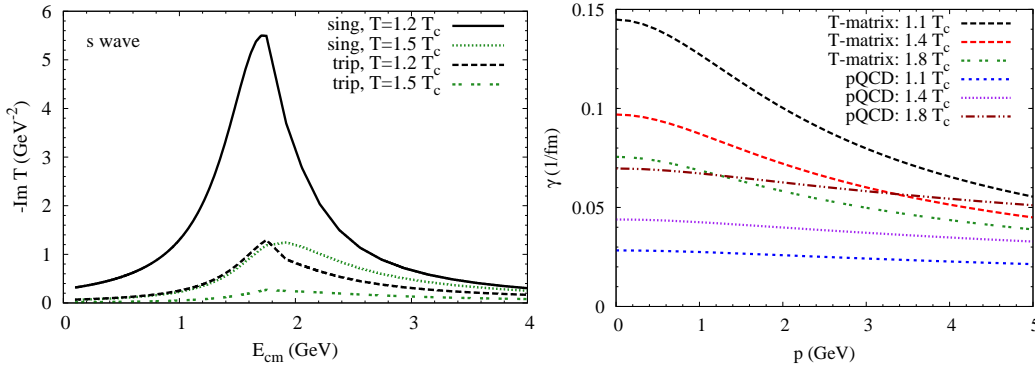


**FIGURE 2.** Left: Imaginary part of the  $S$ -wave in-medium  $T$  matrix for  $c\bar{q}$  and  $cq$  scattering in the color-singlet and -antitriplet channels based on the parameterization of the IQCD potential energy by [Wo]. Right: The drag coefficient,  $\gamma$ , as a function of HQ momentum, calculated via (4) with scattering-matrix elements from the non-perturbative  $T$ -matrix calculation (using the parameterization of the IQCD internal potential energies by [Wo]) compared to a LO perturbative calculation based on matrix elements.

We restrict ourselves to  $S$  ( $l = 0$ ) and  $P$  ( $l = 1$ ) waves. As can be seen from Fig. 2 (left), in the dominating attractive color-singlet  $Q\bar{q}$  and color-antitriplet  $Qq$  channels, close to the critical temperature,  $T_c$ , resonance states close to threshold,  $E_{\text{thr}} = m_Q + m_q$  are formed, similar as conjectured in the effective resonance model described in the previous section [7, 8]. However, in this full in-medium scheme the resonances melt at lower temperatures  $T \gtrsim 1.7 T_c$  and  $T \gtrsim 1.4 T_c$ , respectively.

## HEAVY-QUARK OBSERVABLES IN HEAVY-ION COLLISIONS

A direct comparison between the microscopic description of the HQ dynamics in the QGP and the experimental observables necessitates a dynamical implementation of the HQ scattering in the medium plus a model for the hadronization and finally the implementation of the semileptonic decay.

The HQ motion in the hot and dense QGP, consisting of light quarks and gluons, can be described by a Langevin simulation of the Fokker-Planck equation,

$$\frac{\partial f_Q}{\partial t} = \frac{\partial}{\partial p_i} (p_i \gamma f_Q) + \frac{\partial^2}{\partial p_i \partial p_j} (B_{ij} f_Q). \quad (7)$$

The drag or friction coefficient,  $\gamma$ , and diffusion coefficients,  $B_{ij}$ , are calculated from the invariant scattering-matrix elements [3]. Taking into account elastic scattering of the heavy quark with a light quark or antiquark given in terms of the above calculated  $T$ -matrix one can calculate the drag with a standard procedure the HQ drag and diffusion coefficients, shown in Fig. 2, see Ref. [34] for more details.

The nonperturbative HQ light-quark scattering-matrix elements are supplemented by the corresponding perturbative elastic HQ gluon-scattering ones. The  $t$ -channel singularity is regulated by a gluon-Debye screening mass of  $m_g = gT$  with a strong coupling constant,  $g = \sqrt{4\pi\alpha_s}$ , using  $\alpha_s = 0.4$ .

As shown in Fig. 2, close to  $T_c$  the equilibration times,  $\tau_{\text{eq}} = 1/\gamma \simeq 7 \text{ fm}/c$ , for charm quarks are a factor of  $\sim 4$  smaller than for a corresponding pQCD calculation, reminiscent to the results based on the model assuming  $D$ -meson like resonance states above  $T_c$  [7, 8]. In contrast to this and other calculations of the HQ transport coefficients, here the drag coefficients *decrease* with increasing temperature because of the “melting” of the dynamically generated resonances at increasing temperatures due to the diminishing interaction strength from the lQCD potentials.

To solve the Fokker-Planck equation (7) under conditions of the sQGP medium produced in heavy-ion collisions, we use an isentropically expanding thermal fireball model, assuming an ideal-gas equation of state of  $N_f = 2.5$  effective massless light-quark flavors and gluons. The initial spatial distribution of HQ production is determined with a Glauber model. The  $c$ -quark spectra are taken from a modified PYTHIA calculation to fit  $D$  and  $D^*$  spectra in d-Au collisions [35], assuming  $\delta$ -function fragmentation. The  $b$ -quark  $p_T$  spectrum is taken from PYTHIA assuming a cross-section ratio of  $\sigma_{b\bar{b}}/\sigma_{c\bar{c}} \simeq 5 \cdot 10^{-3}$  and a crossing of the  $c$ - and  $b$ -decay electron spectra at  $p_t \simeq 5 \text{ GeV}$ , consistent with FONLL pQCD calculations [31].

The last step toward a comparison of the above described model for HQ diffusion in the QGP with the  $e^\pm$  data from RHIC is the hadronization of the HQ spectra to  $D$ - and  $B$ -mesons and their subsequent semileptonic decay. Here we use the quark-coalescence model described in [12, 14]. In recent years, the coalescence of quarks in the hot and dense medium created in heavy-ion collisions has been shown to provide a successful hadronization mechanism to explain phenomena such as the scaling of hadronic elliptic-flow parameters,  $v_2$ , with the number of constituent quarks,  $v_{2,h}(p_t) = n_h v_{2,q}(p_t/n_h)$ , where  $n_h = 2(3)$  for mesons (hadrons) denotes the number of constituent quarks contained in the hadron,  $h$ , and the large  $p/\pi$  ratio in Au-Au compared to  $p$ - $p$  collisions [12, 13, 14]. Quark coalescence is most efficient in the low- $p_T$  regime where most  $c$  and  $b$  quarks combine into  $D$  and  $B$  mesons, respectively. To conserve the total HQ number, we assume that the remaining heavy quarks hadronize via ( $\delta$ -function) fragmentation.

As shown in Fig. 3 the Langevin simulation of the HQ diffusion, followed by the combined quark-coalescence fragmentation description of hadronization to  $D$  and  $B$  mesons and their subsequent semileptonic decay, successfully accounts for both the  $R_{AA}$  and  $v_2$  of  $e^\pm$  in 200 AGeV Au-Au collisions [11, 10] at RHIC. The uncertainty due to two different parameterizations of the lQCD potentials by [Wo] [27] and [SZ] [26] is not so large.

Comparing the solid and dashed lines one sees that the effect from the “momentum kick” of the light quarks in coalescence, an enhancement of both  $R_{AA}$  and  $v_2$ , is important for the agreement of both observables with the data. As can be seen from the lower panel in Fig. 3 (right), the effects of the  $B$ -meson decay contribution to the  $e^\pm$  spectra become visible for  $p_T \geq 2.5$ -3 GeV. A closer inspection of the time evolution of the  $p_t$  spectra shows that the suppression of high- $p_T$  heavy quarks occurs mostly in the beginning of the time evolution, while the  $v_2$  is built up later at temperatures close to  $T_c$  which is to be expected since the  $v_2$  of the bulk medium is fully developed at later stages only [37, 38]. This effect is more pronounced due to resonance formation, because the transport coefficients become larger close to  $T_c$ , or at least decrease much slower than in the pQCD case [29].

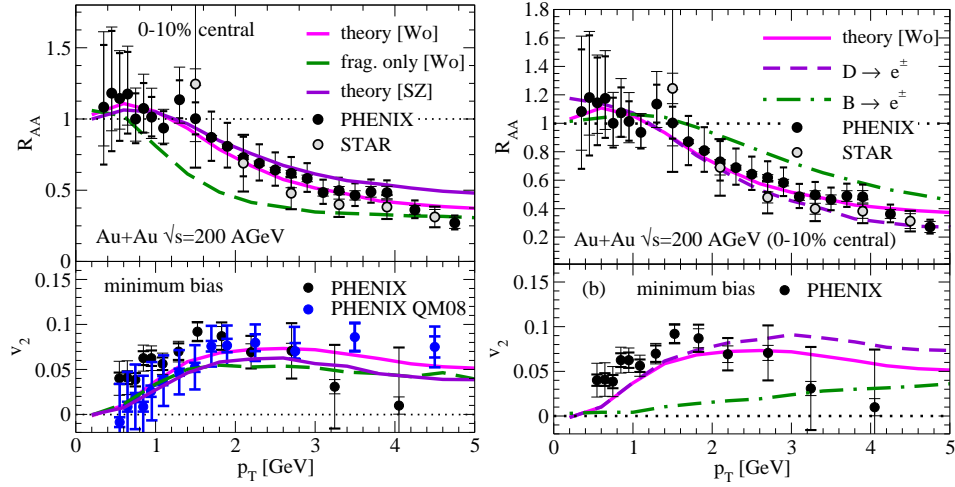


**FIGURE 3.** Left: Results for the nuclear modification factor (upper panel) and elliptic flow (lower panel) of single electrons with/without (solid/dashed lines) quark coalescence in Au-Au collisions compared to RHIC data [10, 11]. Right: As in the left panel but only for the case of [Wo] potential with coalescence included it is shown the contribution of single  $e^\pm$  from D and B decay.

## Prediction at LHC

In 2007 we made predictions for the the  $D$  and  $B$  spectra at the LHC employing the effective resonant model described above. For  $D$  mesons we know that the model is quite reliable in the sense that it generates predictions similar to the  $T$ -matrix approach. Since the initial temperatures at the LHC are expected to exceed the resonance dissociation temperatures, the prediction implemented a switching off of the resonances at  $T_{\text{diss}} = 2T_c = 360$  MeV by a factor  $(1 + \exp[(T - T_{\text{diss}})/\Delta])^{-1}$  with  $(\Delta = 50$  MeV) in the transport coefficients.

The temperature evolution in the fireball assumed a total entropy fixed by the number of charged hadrons which we have extrapolated to  $dN_{ch}/dy \simeq 1400$  for central  $\sqrt{s_{NN}} = 5.5$  TeV Pb-Pb collisions leading to an initial temperature,  $T_0 \simeq 520$  MeV. This multiplicity turns out to be very close to the one measured at  $\sqrt{s_{NN}} = 2.75$  TeV, hence now we know that these have to be considered more properly as predictions for this energy.

Initial HQ  $p_T$  spectra are computed using PYTHIA with parameters as used by the ALICE Collaboration [36]. Hadronization is treated as previously discussed for the RHIC case. The shadowing has not been included but as shown by the orange solid line this should not affect the prediction at  $p_T > 3.5$  GeV.

In Fig. 4 the predictions for the  $D$ -meson  $R_{AA}$  are shown by the shaded red area corresponding to the uncertainties in the resonance model. The data from the ALICE Collaboration [6] are shown by rectangles, red for  $D^+$  and green for  $D^0$ , and are for the 0 – 20% centrality and therefore corresponding to an impact parameter,  $b = 4.7$  fm, hence more central with respect to the 2007 calculations. For this reason in the figure the red dashed line is drawn to indicate the extrapolation from the  $b = 7$  fm calculation to the more central with  $b = 4.7$  fm which results in a 15% correction. It is clear that



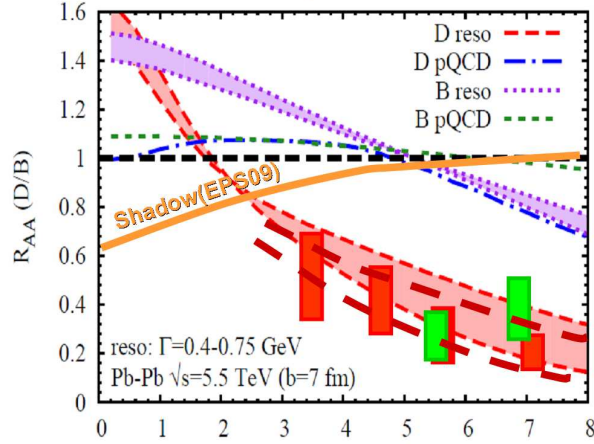


**FIGURE 4.** The nuclear modification for  $D$  meson at LHC for  $Pb + Pb$  at  $\sqrt{s_{NN}} = 2.75$  TeV for more detail see the text.

the prediction from simple pQCD elastic scattering, shown by the blue dash-dotted line, cannot account at all for the observed suppression of the  $D$  spectra.

Data with a better statistics and especially a measurement of the elliptic flow will greatly improve the discrimination power of the model. From the theoretical side it is desirable to have predictions using the  $T$ -matrix approach based on the IQCD-based potential, especially for the  $B$  mesons. These are differently affected by the medium and should show a resonant scattering persistent up to higher temperatures compared to the  $D$  mesons resulting in a smaller  $R_{AA}$  compared to the simplified resonance model shown by the violet shaded area shown in Fig. 4.

## CONCLUSIONS

The in-medium interaction of heavy quarks have been intriguing from the first preliminary results at RHIC showing a much larger suppression than expected, together with a large elliptic flow, as inferred from semileptonic HQ decay electrons. An in-medium  $T$ -matrix approach (utilizing potentials estimated from lattice QCD) has been applied to evaluate HQ interactions in the QGP showing the existence of in medium prehadronic and diquark resonance states, which increase in strength when approaching  $T_c$ . When implemented into Langevin simulations at RHIC, reasonable agreement with both the suppression and elliptic flow of  $e^\pm$  spectra from HQ decays emerges.

Several theoretical problems remain open like a proper definition of the potential, corrections to the  $T$ -matrix approach including radiative ones, in-medium mass and width effects as well as a self-consistent treatment of the hadronization via coalescence. On the other hand this field is entering a new stage thanks to the possibility to disentangle the  $B$  and  $D$  mesons which in itself can provide the key to discriminate different models [16, 17, 18, 39, 40].

## ACKNOWLEDGMENTS

VG is supported by the MIUR under the Firb Research Grant RBFR0814TT and by the ERC-StG2010 under the QGPDyn Grant n.259684. RR is supported by the US National Science Foundation under grant no. PHY-0969394 and by the A.-v.-Humboldt foundation.

## REFERENCES

1. S. Borsanyi *et al.*, JHEP **1011**, 077 (2010)
2. V. Greco, C. M. Ko, R. Rapp, Phys. Lett. **B595** (2004) 202-208.
3. Svetitsky B 1988 Phys. Rev. D **37** 2484
4. N. Armesto *et al.*, Phys. Lett. B **637**, 362 (2006)
5. S. Wicks, W. Horowitz, M. Djordjevic, and M. Gyulassy, Nucl. Phys. A **784**, 426 (2007)
6. Plenary Session Talk at Quark Matter 2011, 22-28 May, Annecy (France): *Heavy-flavor production in PbPb collisions at the LHC measured with the ALICE detector*;
7. H. van Hees and R. Rapp, Phys. Rev. C **71**, 034907 (2005)
8. H. van Hees, V. Greco, and R. Rapp, Phys. Rev. C **73**, 034913 (2006)
9. N. Armesto, A. Dainese, C. A. Salgado, U. A. Wiedemann, Phys. Rev. **D71** (2005) 054027.
10. B. I. Abelev *et al.* (STAR Collaboration), Phys. Rev. Lett. **98**, 192301 (2007)
11. A. Adare *et al.* (PHENIX Collaboration), Phys. Rev. Lett. **98**, 172301 (2007)
12. V. Greco, C. M. Ko, P. Levai, Phys. Rev. **C68** (2003) 034904.
13. R. J. Fries, B. Müller, C. Nonaka, and S. A. Bass, Phys. Rev. C **68**, 044902 (2003);
14. V. Greco, Eur. Phys. J. ST **155** (2008) 45-59.
15. R. J. Fries, V. Greco, P. Sorensen, Ann. Rev. Nucl. Part. Sci. **58** (2008) 177-205.
16. H. van Hees, M. Mannarelli, V. Greco, and R. Rapp, Phys. Rev. Lett. **100**, 192301 (2008)
17. P. B. Gossiaux, J. Aichelin, Phys. Rev. **C78** (2008) 014904.
18. W. M. Alberico *et al.*, Eur. Phys. J. **C71** (2011) 1666.
19. M. Asakawa, T. Hatsuda, Phys. Rev. Lett. **92**, 012001 (2004), Nucl. Phys. **A721**, 869 (2003).
20. G. Aarts, S. Kim, M. P. Lombardo, M. B. Oktay, S. M. Ryan, D. K. Sinclair, J. -I. Skullerud, Phys. Rev. Lett. **106** (2011) 061602; G. Aarts, C. Allton, S. Kim, M. P. Lombardo, M. B. Oktay, S. M. Ryan, D. K. Sinclair, J. -I. Skullerud, [arXiv:1109.4496 [hep-lat]].
21. M. Mannarelli and R. Rapp, Phys. Rev. C **72**, 064905 (2005)
22. S. Godfrey and N. Isgur, Phys. Rev. D **D32**, 189 (1985)
23. M. Avila, Phys. Rev. D **49**, 309 (1994)
24. O. Kaczmarek, F. Karsch, P. Petreczky, and F. Zantow, Nucl.Phys.Proc.Suppl. **129**, 560 (2004)
25. O. Kaczmarek and F. Zantow (2005), arXiv:hep-lat/0506019
26. E. V. Shuryak and I. Zahed, Phys. Rev. D **70**, 054507 (2004)
27. C.-Y. Wong, Phys. Rev. C **72**, 034906 (2005)
28. M. Döring *et al.*, Phys. Rev. D **75**, 054504 (2007).
29. F. Riek and R. Rapp, Phys. Rev. C **82** (2010) 035201.
30. R. Rapp and H. van Hees (2008), arXiv:0803.0901 [hep-ph]
31. M. Cacciari, P. Nason, R. Vogt, Phys. Rev. Lett. **95** (2005) 122001.
32. S. Abreu, *et al.*, J. Phys. G **G35** (2008) 054001.
33. P. Petreczky and K. Petrov, Phys. Rev. D **70**, 054503 (2004)
34. R. Rapp, D. Blaschke, P. Crochet, Prog. Part. Nucl. Phys. **65** (2010) 209.
35. J. Adams *et al.* (STAR Collaboration), Phys. Rev. Lett. **94**, 062301 (2005)
36. G. Alessandro, (Ed.) *et al.* [ ALICE Collaboration ], J. Phys. G **G32** (2006) 1295-2040.
37. R. Rapp, J. Phys. G **36** (2009) 064014
38. F. Scardina, M. Di Toro, V. Greco, Phys. Rev. **C82** (2010) 054901.
39. J. Uphoff, O. Fochler, Z. Xu, C. Greiner, Phys. Rev. **C84** (2011) 024908.
40. M. He, R.J. Fries and R. Rapp, arXiv:1106.6006 [nucl-th].